

# Laser weldability of Pt and Ti alloys

N.J. Noolu<sup>a,\*</sup>, H.W. Kerr<sup>a</sup>, Y. Zhou<sup>a</sup>, J. Xie<sup>b</sup>

<sup>a</sup> Center for Advanced Materials Joining, University of Waterloo, Waterloo, Canada

<sup>b</sup> Cardiac Rhythm Management Division, Street Jude Medical Inc., Sylmar, CA, USA

Received 6 July 2004; received in revised form 16 December 2004; accepted 23 December 2004

## Abstract

Crack susceptibility of laser spot welds between Pt and Ti alloys was studied by characterizing the surface and the cross-sections of the welds produced at different pulse energies. Increase in laser pulse energy increased the dilution by the Ti alloy, giving rise to the evolution of microstructures with varying Ti contents across the entire fusion zone. Hardness results showed that regions with 66–75% Ti, i.e. consisting of primary  $Ti_3Pt$  and/or  $Ti_3Pt + TiPt$  eutectic, have a hardness higher than 700 Vickers hardness numbers (VHN), while regions with 42–66% Ti, i.e. consisting of primary  $TiPt$ , possessed hardness between 400 and 700 VHN. The extent of cracking increased with the increase in pulse energy and the cracked regions consisted of Ti contents between 50 and 75%. Brittle cracking in microstructures consisting of  $Ti_3Pt$  and  $TiPt$  phases suggested that one or both of the constituent phases are susceptible to cracking. However, crack arrest in microstructures predominantly consisting of  $TiPt$  showed that  $Ti_3Pt$  is the most susceptible phase to cracking in Pt–Ti alloy welds.

© 2005 Published by Elsevier B.V.

**Keywords:** Pt–Ti; Weldability; Crack susceptibility; Medical applications; Intermetallics

## 1. Introduction

Laser welding has been used as one of the major manufacturing processes in the medical device industry because it offers number of advantages such as precision and non-contact processing, with a small HAZ, consistent and reliable joints etc. [1]. Laser welding has been used to produce many kinds of medical products such as pacemakers, defibrillators, catheters, cochlear, insulin pumps, stents, and orthopedic implants [2]. For implantable devices, biocompatible metals and alloys such as titanium, nitinol, cobalt-based alloys, stainless steel, platinum, and niobium, must be used. However, laser weldability of these materials, especially dissimilar material combinations, is still poorly understood. One the extensively used material combinations in implantable medical devices, but very rarely reported, is laser welding of platinum alloys to titanium alloys.

High strength, low weight, outstanding corrosion resistance, and bio-compatibility make Ti and its alloys suitable for medical devices such as pacemakers and defibrillators. Excellent electrical conductivity, durability, biological compatibility, and oxidation resistance make the Pt–Ir wires well suited for electrodes in these medical components [3]. Although good mechanical and electrochemical properties are required, the primary purpose of joining the Pt alloy wire to the Ti alloy component in medical devices is to form an electrical connection. However, electrical conductivity along with corrosion and mechanical properties of a weld joint are primarily dependent on the structure and properties of the fusion zone. Cracking in Pt–Ti alloy welds is a problem. The medical industry is investigating to improving the integrity of these joints by process modifications and evaluation of alternative materials. Although it has been reported that Pt–Ti welds are brittle in nature [2], to the authors' knowledge, no previous study of the effects of weld process conditions on Pt–Ti alloy weld quality has been published to understand the properties of these weld joints. An examination of the Pt–Ti phase diagram [4] in Fig. 1 shows that various intermetallic phases ( $Ti_3Pt$ ,  $TiPt$ ,  $Ti_3Pt_5$ ,  $TiPt_3$ , etc.) can form between

\* Corresponding author. Tel.: +1 480 552 7802.

E-mail addresses: [nnoolu@mecheng1.uwaterloo.ca](mailto:nnoolu@mecheng1.uwaterloo.ca),  
[narendra.j.noolu@intel.com](mailto:narendra.j.noolu@intel.com) (N.J. Noolu).

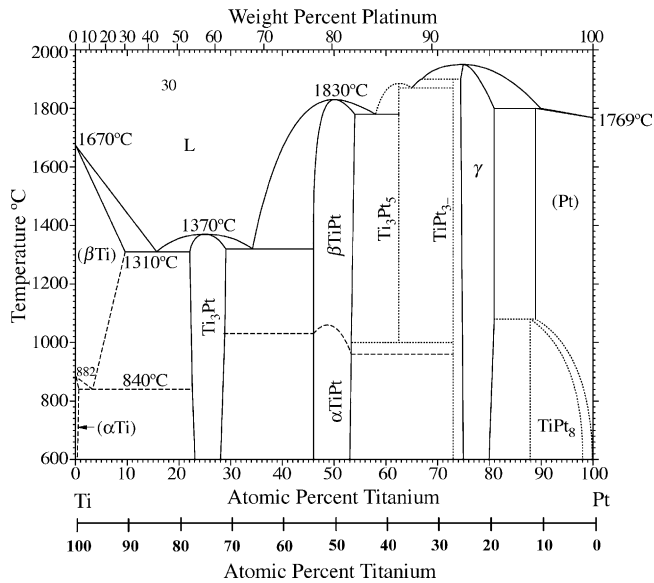


Fig. 1. Binary phase diagram showing the possible phases between Pt and Ti [2].

Pt and Ti and could possibly affect the weldability between their alloys. The purpose of the present study is to gain an understanding of the weldability of laser spot welds between Pt and Ti alloys.

## 2. Experimental methods

Single pulsed laser spot welds were produced between Pt–10Ir wire of 400  $\mu\text{m}$  diameter and Ti–6Al–4V component of 1 mm thickness by varying the laser pulse energy between 6 and 10 J, but at a constant pulse time of 6 ms. Prior to welding, the specimens were soaked in acetone, then in methanol, and dried in air. They were assembled in the configuration shown in Fig. 2, with the laser beam at 75° to the surface of the Ti alloy component to avoid laser back reflection. The Pt alloy wire was held down onto the Ti alloy component using a one-sided tape. The laser was focussed on the surface of the Ti alloy component and welding was performed with a Lumonics JK 702H pulsed Nd:YAG laser with a Gaussian

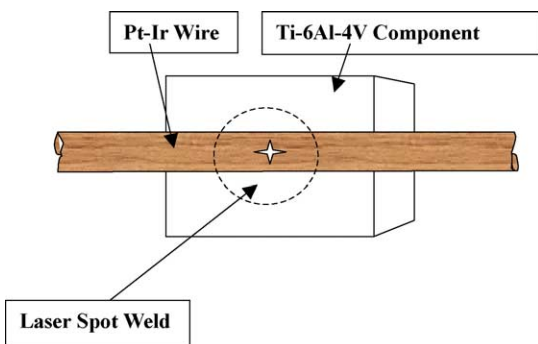


Fig. 2. Geometry of Pt alloy wire and Ti alloy component prior to welding.

beam distribution and a spot size of about 413  $\mu\text{m}$  [5]. Argon shielding gas at 30 cfh flow rate through a nozzle of 8 mm inner diameter, 6 mm above the Ti alloy component and at about 75° to its surface, was used to minimise atmospheric contamination.

After welding, the surface of each spot weld was examined for possible cracks, and quantitatively analyzed for compositional variations using energy dispersive spectroscopy (EDS) in a scanning electron microscope (SEM). Analysis of the microstructures was performed on a LEO 1530 field emission scanning electron microscope (FESEM) equipped with EDAX Genesis 2000. The quantitative data was collected at 20 or 21 KV accelerating voltage selecting L peaks to resolve and quantify Pt and Ir contents and K peaks to quantify Al, V and Ti contents. It should be noted that the compositions given are always in atomic proportions, unless otherwise mentioned and the microstructural constituents were predicted based solely on their Pt and Ti contents.

The welds were then cold mounted and metallographically polished for further observations of the microstructure and possible cracks in the weld cross-sections. Microhardness indenting (load of 50 gf, time of 15 s) was performed on a Shimadzu hardness tester after which diagonals of the indentations were measured in an optical microscope and Vickers hardness numbers (VHN) were obtained using Image Pro (Version 4.5) software.

## 3. Results and discussion

### 3.1. Microstructural evolution

Increases in laser pulse energy not only resulted in larger Pt–Ti alloy welds, but also higher dilution by the Ti alloy base metal giving rise to an evolution of the fusion zone microstructure. Weld cross-sections in Fig. 3 are examples showing the effect of pulse energy on the dilution of the fusion zone by the Ti alloy base metal. The cross-section of the weld produced with 6 J pulse energy in the back scattered electron image of Fig. 3(a) shows extensive regions of bright contrast in the fusion zone and hence, has minimal dilution by the Ti alloy. The increase in regions of grey contrast evident in the back scattered electron images of the fusion zones in Fig. 3(b) and (c) of 8 and 10 J welds, respectively, indicates that higher laser pulse energy increases the dilution by the Ti alloy base metal.

Fig. 4(a) and (b) shows the variation of Ti content (% Ti/(Ti + Pt)) from the Pt alloy base metal side to the Ti alloy base metal end of the fusion zones produced at 8 and 10 J pulse energies, respectively. Fig. 4(a) also shows that about two-thirds of the regions analyzed by the line scan across the 8 J weld cross-section consist of 38–50% Ti, while the rest of the regions on the line scan, which are near the Ti alloy, consist of 50–75% Ti. However, the line scan across the 10 J weld cross-section in Fig. 4(b) shows that most of the regions analyzed consist of 50–75% Ti. The length of line scans on

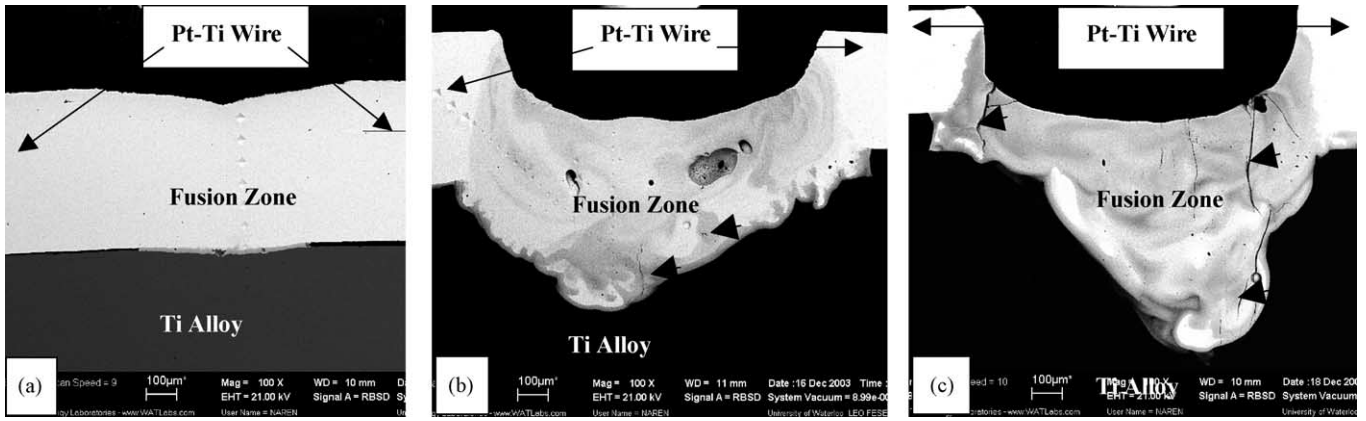


Fig. 3. Back scattered electron images showing the effect of (a) 6, (b) 8, and (c) 10 J pulse energy on the evolution of regions of grey contrast. The dark arrows show regions of grey contrast.

8 and 10 J weld cross-sections, were about 600 and 750  $\mu\text{m}$ , respectively. It can also be observed in Fig. 4(a) and (b) that regions of grey contrast have a Ti content of 50% or higher and as shown in Fig. 3, these regions increase with pulse energy.

In a preliminary study [6] of Pt–Ir alloy welding to Ti–6Al–4V and commercially pure Ti (CP grade 2), there were no observable differences in the nature of cracking and the extent of dilution. This result suggests that Al and V do not significantly influence the cracking tendency in these welds. The EDS results showed that Ir partitions to Pt rich regions, and the complete solubility between Pt and Ir in bi-

nary solutions [4], suggests that eutectic points of the Pt–Ti diagram should be shifted only by a few percent. Based on these considerations, an analysis purely based on Pt–Ti binary system is considered to yield reasonable interpretation. Hence, only Pt and Ti atomic contents from EDS analysis were employed, to simplify the analysis in predicting the constituent phases of the weld microstructures. Based on the Pt–Ti phase diagram, regions with 66–75% Ti consist of primary  $\text{Ti}_3\text{Pt}$  and/or  $\text{Ti}_3\text{Pt} + \text{TiPt}$  eutectic, while 50–66% Ti consist of primary TiPt and/or  $\text{Ti}_3\text{Pt} + \text{TiPt}$  eutectic. Similarly, regions with 38–50% Ti consist of primary TiPt, primary  $\text{Ti}_3\text{Pt}_5$ , and/or their eutectic. Comparing Fig. 4(a) and

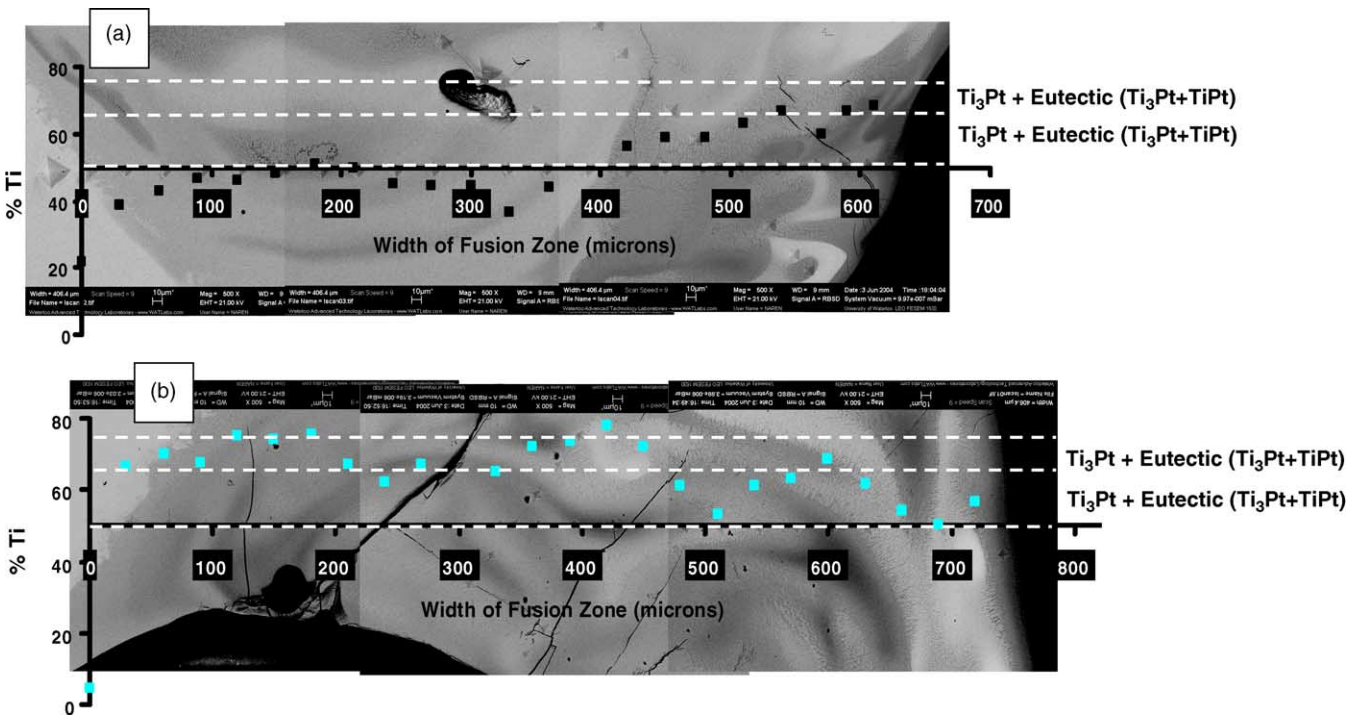


Fig. 4. Variation of Ti content (% Ti) across the fusion zone of welds produced with (a) 8 and (b) 10 J pulse energy, respectively. X-axis represents the horizontal line along which EDS spot analysis of the microstructures shown in the background was performed. Possible phases that can form between 66–75% and 50–66% Ti contents are indicated between the respective dashed lines.

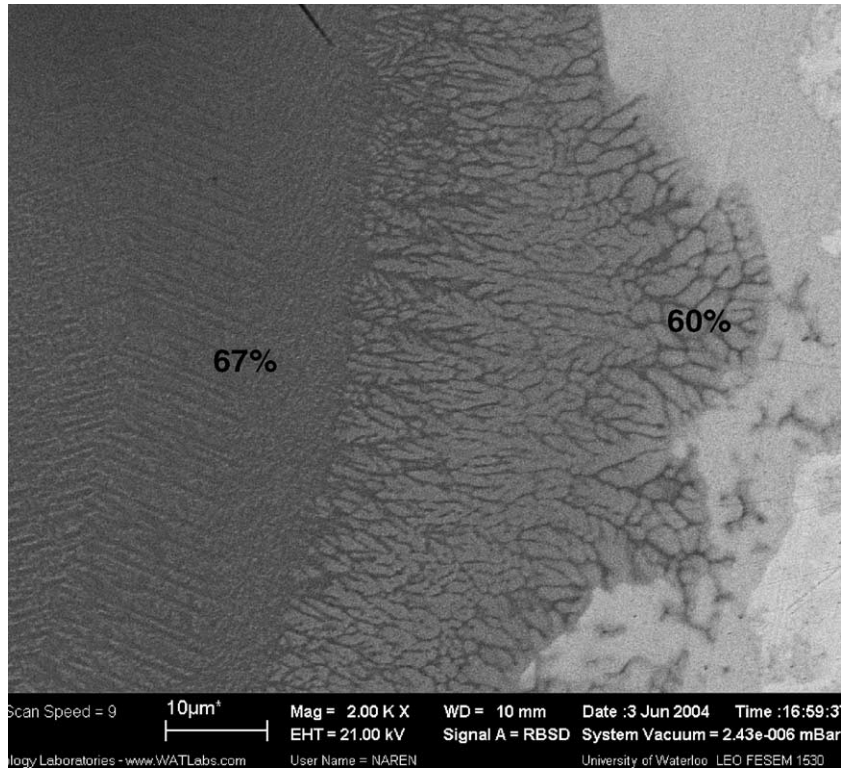


Fig. 5. Back scattered electron image showing typical microstructure in a region of grey contrast. The region with 67% Ti represents a microstructure predominantly consisting of the  $Ti_3Pt + TiPt$  eutectic, while the region with 60% Ti represents a microstructure with primary  $TiPt$  and  $Ti_3Pt + TiPt$  eutectic.

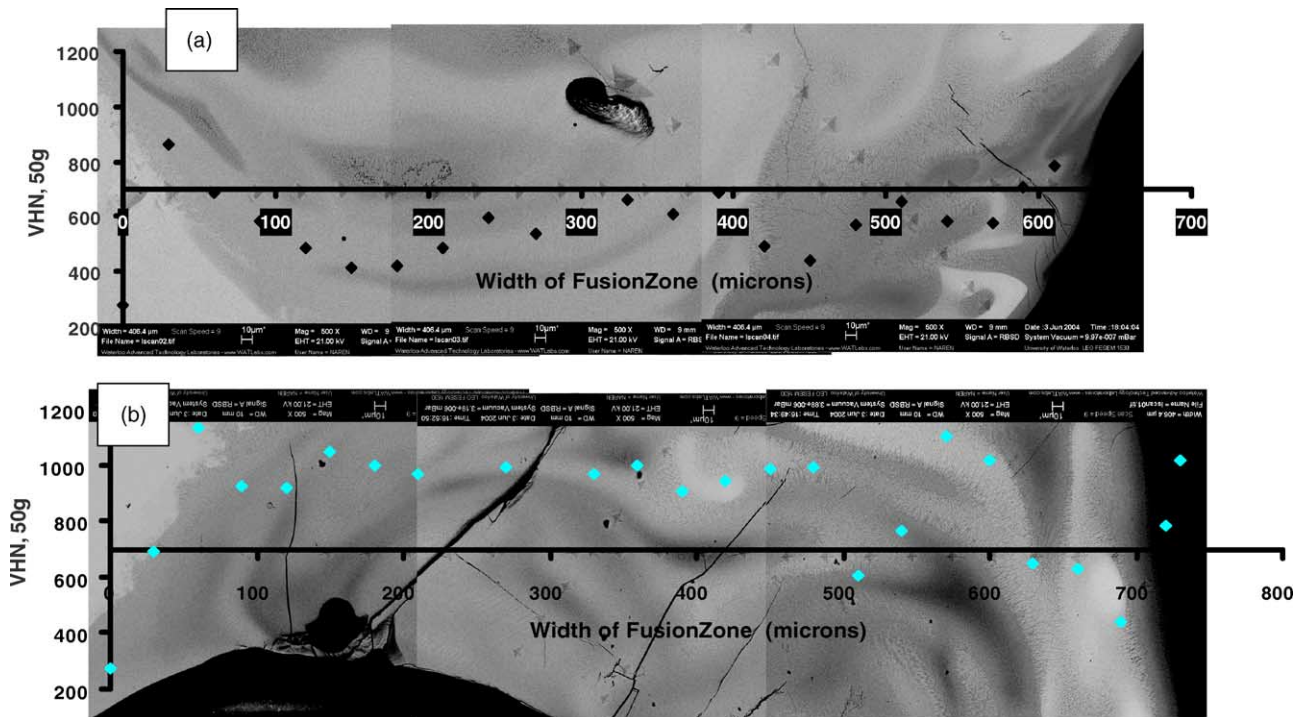


Fig. 6. Variation in hardness across the fusion zone of welds produced with (a) 8 and (b) 10J pulse. Hardness indenting and EDS spot analysis (Fig. 4 were performed at the same locations along the horizontal lines represented by the X-axis of the plots. The background microstructures shown are back scattered electron images across the fusion zone.

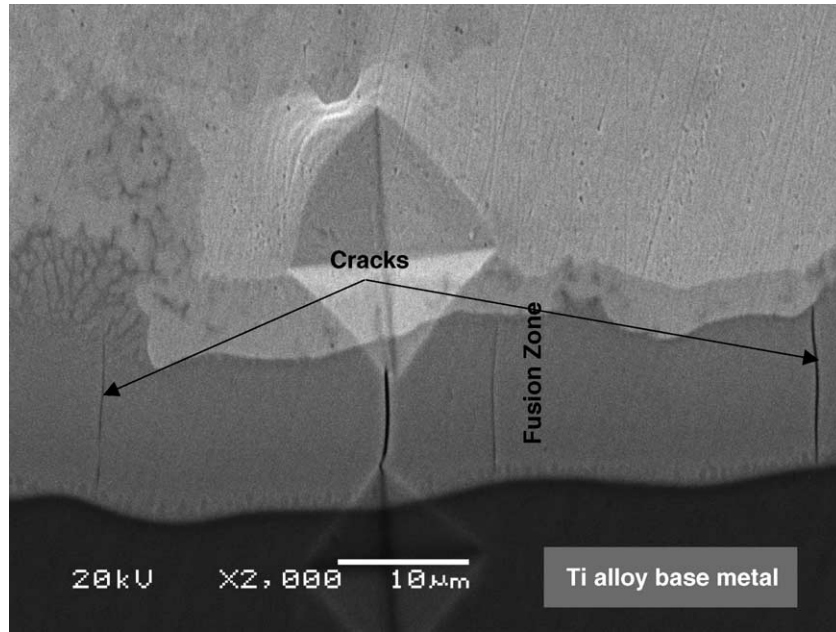


Fig. 7. Secondary electron image showing crack propagation in the regions of fusion zone very close to the Ti alloy base metal in a 6 J weld.

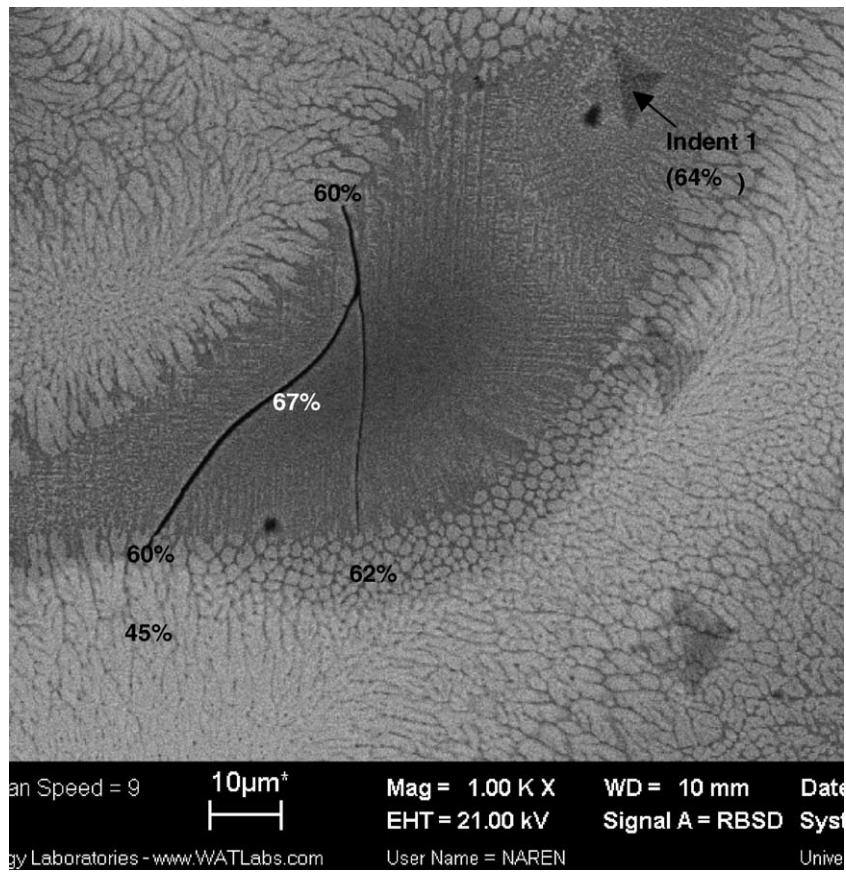


Fig. 8. Back scattered electron image showing crack propagation through a region with 67% Ti and its arrest in regions with Ti content of 62% or less.

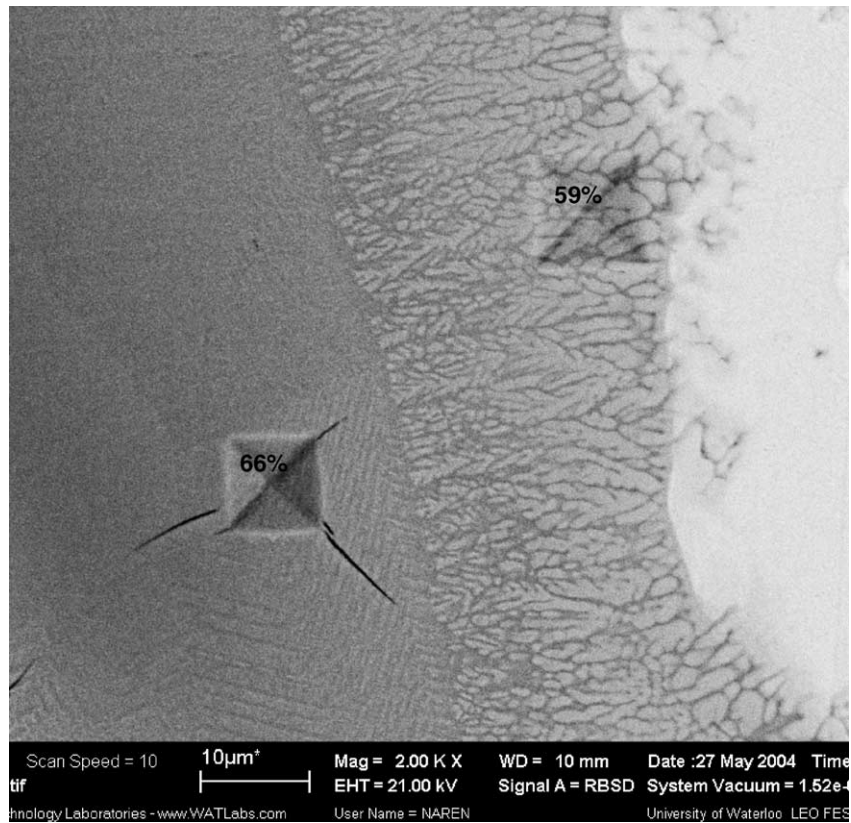


Fig. 9. Back scattered electron image showing hardness indentations in a microstructure similar to that in Fig. 5 with their respective Ti contents.

(b) it can also be observed that the length of regions on the line scan that consisted of primary  $\text{Ti}_3\text{Pt}$ , primary  $\text{TiPt}$  and/or  $\text{Ti}_3\text{Pt} + \text{TiPt}$  eutectic, i.e. with 50–75% Ti, was about 200  $\mu\text{m}$  in the 8 J weld fusion zone, while these regions were spread over the entire linescan across the 10 J weld fusion zone.

The EDS line scan results suggest that the growth of regions constituting of primary  $\text{Ti}_3\text{Pt}$ , primary  $\text{TiPt}$  and/or their eutectic mixture is restricted to the vicinity of the Ti alloy base metal in 8 J welds, and an increase in pulse energy to 10 J promotes growth of these phases across the entire weld fusion zone. Accordingly, the SEM examinations revealed microstructures consisting of  $\text{Ti}_3\text{Pt}$ ,  $\text{TiPt}$ , and/or  $\text{Ti}_3\text{Pt} + \text{TiPt}$  eutectic in the vicinity of the Ti alloy base metal in the 8 J weld, but widespread in the 10 J weld. Fig. 5 is an example of a region in a fusion zone with different Ti contents, but consisting of  $\text{Ti}_3\text{Pt}$  and  $\text{TiPt}$  phases. The Pt–Ti phase diagram suggests that the region with 60% Ti consists of primary  $\text{TiPt}$  and  $\text{Ti}_3\text{Pt} + \text{TiPt}$  eutectic, while the region with 67% Ti consists primarily of  $\text{Ti}_3\text{Pt} + \text{TiPt}$  eutectic.

### 3.2. Hardness of the fusion zone microstructures

Fig. 6 compares the hardness profiles of the fusion zones produced with 8 and 10 J pulse energies and shows the effect

of pulse energy on the evolution of hard microstructures. The hardness results in Fig. 6(a) indicate that most of the 8 J weld fusion zone was softer than 700 VHN and that only in the vicinity of the Ti alloy base metal were there regions harder than 700 VHN. However, the hardness profile of Fig. 6(b) suggests that the entire 10 J weld fusion zone was harder than 700 VHN. It should be noted that EDS line scans and the hardness indenting were performed along the same length of the weld cross-section, and hence the data from the two analyses can be directly correlated. Comparison of Figs. 4 and 6 shows that regions with 66–75% Ti, i.e. comprised of primary  $\text{Ti}_3\text{Pt}$ , were harder than 700 VHN. Regions with 42–66% Ti, i.e. consisting of primary  $\text{TiPt}$ , possessed hardness between 400 and 700 VHN. It is evident that 10 J pulse energy promoted wide growth of microstructures harder than 700 VHN. Based on the hardness values of regions with 50–75% Ti, it can be inferred that microstructures with  $\text{Ti}_3\text{Pt}$  and/or  $\text{TiPt}$  are hard in nature. In comparison, the hardness values of commercially pure Pt and Ti are 40 and 160–220 VHN [7,8], respectively.

### 3.3. Crack Susceptibility of Pt–Ti Alloy Welds

Irrespective of the pulse energy, cracks were observed in the fusion zone of all welds. In addition, the extent of cracking

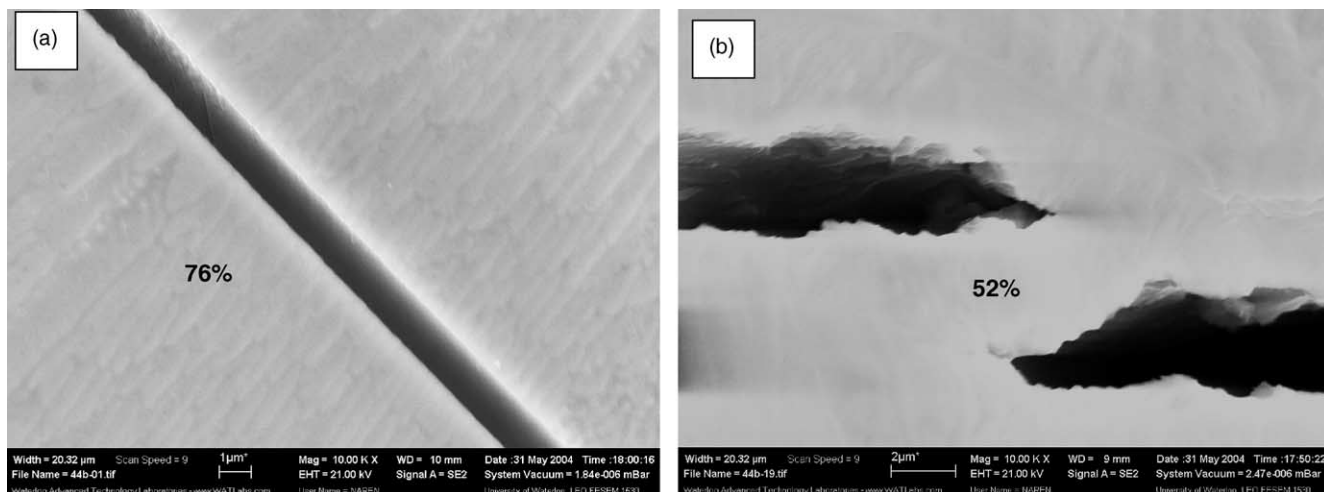


Fig. 10. Secondary electron images from the surface of a 10J spot weld showing the nature of cracking across microstructures with Ti contents of (a) 76 and (b) 57%. Seventy seven percent Ti suggests the predominant presence of  $\text{Ti}_3\text{Pt}$  while that with 57% Ti suggests the predominant presence of  $\text{TiPt}$ .

increased with increases in the pulse energy, in accordance with the increase in dilution by the Ti alloy base metal. Evident in Fig. 7, cracking was restricted to regions very close to the Ti alloy base metal in the 6J weld fusion zone. As shown by arrows in Fig. 3(a) and (b), with increases in pulse energy to 8 and 10J, cracks were observed over increasing distances, beginning near the Ti alloy base metal. It is also evident in Fig. 3, that the cracks were always associated with regions of grey contrast. The wider the growth of the regions of grey contrast, the higher was the extent of cracking. As mentioned in Section 3.1, these regions of grey contrast typically had 50–75% Ti and as shown in Fig. 5, consisted of  $\text{TiPt}$  and  $\text{Ti}_3\text{Pt}$  phases.

Fig. 8 shows a crack in the fusion zone and illustrates the importance of the Ti content on the crack susceptibility of microstructures. A hardness of 997 VHN in the region of grey contrast (indent 1 adjacent to the crack shown in Fig. 8) suggests that the grey region is very hard. A Ti content of about 67% in these regions suggests a microstructure predominantly consisting of  $\text{Ti}_3\text{Pt} + \text{TiPt}$  eutectic and the presence of cracks shows that this microstructure is susceptible to cracking. In addition, the crack arrest at the transition of microstructure from the predominantly eutectic mixture to the primary  $\text{TiPt}$ , in Fig. 8, suggests that  $\text{Ti}_3\text{Pt}$  is the primary susceptible phase to cracking. In Fig. 9, cracking occurs around the hardness indentations in the region with 66% Ti, but not in the region with 59% Ti, which corroborates the importance of  $\text{Ti}_3\text{Pt}$  on cracking.

An examination of the surface of the spot welds revealed the fractured surfaces of cracks in the weld microstructures. Although occasional presence of solidification cracks was noted, the nature of cracking was predominantly transgranular, and their morphology suggests that they are solid-state in nature. Fig. 10 shows cracking across microstructures with Ti contents of (a) 76%, and (b) 52%. From the binary phase diagram, regions with 76% Ti consist predominantly of pri-

mary  $\text{Ti}_3\text{Pt}$ , while regions with 52% Ti consist mainly of primary  $\text{TiPt}$ . These images show that the crack path across microstructures consisting of primary  $\text{Ti}_3\text{Pt}$  is flat, while the crack propagation across the microstructure consisting of primary  $\text{TiPt}$  is arrested. These results again suggest that  $\text{Ti}_3\text{Pt}$  is brittle and the most susceptible phase for cracking in the Pt–Ti weld fusion zone.

$\text{Ti}_3\text{Pt}$  belongs to a group of intermetallic compounds with A15 structure [9]. Not only do A15 compounds exhibit ductile-to-brittle transition temperatures as high as 1400 °C [10], they generally do not exhibit any plastic deformation under ambient conditions [11]. The yield strengths of these compounds are very high even at elevated temperatures [12] and the deformation is limited due to limited operating slip systems [10]. The experimental observations of a flat crack path through  $\text{Ti}_3\text{Pt}$  (for example in Fig. 10(a)) are in agreement with the low ductility of A15 compounds. Hence, it is suggested that microstructures consisting predominantly of  $\text{Ti}_3\text{Pt}$  possess low ductility and have high susceptibility to cracking.

#### 4. Summary

The present study examined the cracking tendency of laser spot welds joining Pt-based wire to a Ti-based component. Increases in pulse energy caused increased dilution by the Ti alloy. Within the range of pulse energies studied, the higher the dilution by the Ti alloy base metal, the wider was the growth of microstructures with  $\text{Ti}_3\text{Pt}$  and  $\text{TiPt}$  phases and the harder were the microstructures. In addition, extensive growth of microstructures with  $\text{Ti}_3\text{Pt}$  and  $\text{TiPt}$  phases resulted in more cracks. Observations of cracks in microstructures that predominantly consist of primary  $\text{Ti}_3\text{Pt}$  and its eutectic with  $\text{TiPt}$  suggest that  $\text{Ti}_3\text{Pt}$  is the primary phase responsible for cracking in these Pt–Ti alloy welds.

## Acknowledgements

Thanks are due to Jian Zhang and Dr. Xiaogang Li for helping with the production of the weld samples. The help of Prof. W.H.S. Lawson in reviewing the manuscript is also appreciated.

## References

- [1] ASM Handbook, vol. 6, ASM International, Materials Park, OH, 1997.
- [2] J. Xie, S. Safarevich, in: S. Shrivastava (Ed.), Proceedings of the Materials and Processes for Medical Devices Conference, 8–19 September, Anaheim, CA, ASM International, 2003, pp. 25–30.
- [3] Website: <http://www.platinum.matthey.com/applications/medical.html>.
- [4] T.B. Massalski (Ed.), Binary Alloy Phase Diagrams, ASM International, Materials Park, OH, 1990.
- [5] E. Biro, Y. Zhou, D.C. Weckman, J. Laser Appl. 13 (3) (2001) 96.
- [6] Microjoining laboratory, University of Waterloo, Unpublished work, 2004.
- [7] [http://www.noble.matthey.com/library/Platinum%20Jewellery%20Alloys\\_brochure\\_English\\_114.pdf](http://www.noble.matthey.com/library/Platinum%20Jewellery%20Alloys_brochure_English_114.pdf).
- [8] <http://www.euro-titan.com/pdf/surface.pdf>.
- [9] W.B. Pearson, A Handbook of Lattice Spacings and Structures of Metals and Alloys, Pergamon Press, 1958.
- [10] D.M. Shah, D.L. Anton, Mater. Sci. Eng. A153 (1992) 402.
- [11] L.R. Eisenstatt, R.N. Wright, Metall. Trans. A vol. 11A (1980) 1131.
- [12] S. Mahajan, J.H. Wernick, G.Y. Chin, S. Nakahara, T.H. Geballe, Appl. Phys. Lett. 33 (11) (1978) 972.